Red edge spectral characteristics of Hudson Bay coastal vegetation

Samantha Fraser
Department of Geography, University of Winnipeg

Jeremy Sewell
Department of Geography, University of Winnipeg

Joni Storie
Department of Geography, University of Winnipeg

Adrian Werner
Department of Geography, University of Winnipeg

Charles Enns
Department of Geography, University of Winnipeg

Genevieve Berard
Department of Geography, University of Winnipeg

Improving the discrimination of coastal vegetation with remotely sensed imagery is needed for accurate mapping of shoreline position to determine sea level changes. Homogeneous vegetation cover can be successfully discriminated using remotely sensed data. However, the key to improving coastal vegetation mapping is better detection of heterogeneous vegetation cover. The focus of this article is to explore the relationship between vegetation cover amounts (homogeneous, heterogeneous) with remotely sensed visible-infrared spectra to improve mapping of coastal vegetation. This goal is achieved by quantifying the relationship between plant area index (PAI) values and change from homogeneous and heterogeneous vegetation cover. If PAI values can be used as an indicator for vegetation cover, then the statistical relationship between the PAI values and the first derivative of the red edge in the hand-held spectra can be determined. Results showed that the PAI values were statistically different for the two vegetation zones and thus PAI can be used as an indicator. Significant linear relationships were found between PAI values and the first derivative with the best correlation obtained using the amplitude characteristics (R2~0.90) for both vegetation zones. A negative correlation was found for the PAI spectra in the homogeneous vegetation while a positive correlation was found for the PAI spectra in the heterogeneous zone. It was concluded that spectral discrimination between homogeneous and heterogeneous vegetation is possible when using the first derivative of the red edge. The next step is to incorporate spectral information into an object-based classification to improve coastal vegetation mapping.

Keywords: wetlands, hydrology, remote sensing, coastal, shoreline mapping

Correspondence to: Joni Storie, Department of Geography, University of Winnipeg, 515 Portage Avenue, Winnipeg, MB R3B 2E9
Email: *j.storie@uwinnipeg.ca*

Introduction

This article investigates the spectral difference between homogeneous and heterogeneous vegetation near Churchill, Manitoba for the purpose of improving coastal vegetation mapping using remotely sensed data. This is the first phase of a larger project aimed to use the transition from homogeneous to heterogeneous vegetation as a detectable, stable feature for geocoding remotely sensed images. If a reliable geocoding feature can be detected, this would improve change detection of shoreline position using multi-temporal images. Subarctic coastal vegetation has a short growing season (late June to September) and, as a result, the distribution and composition of vegetation changes little from year to year. The stability of coastal vegetation means that it may be useful as a geocoding feature compared to geomorphic shoreline features which experience annual erosion and deposition changes due to yearly sea ice on Hudson Bay.

The boundary between the change from homogeneous to heterogeneous vegetation is defined as the decrease in vegetation percent cover from homogeneous vegetation (100% cover) to heterogeneous vegetation (<90% cover). This change was observed in the field and statistically validated based on change in plant species, percent cover and elevation (Werner et al. in press). In remote sensing literature, the terms 'homogeneous' and 'heterogeneous' are used to describe the amount of vegetation cover or amount of vegetation type (Bartlett and Klemas 1980; Curran 1980; Asner and Heidebrecht 2002). In this article, homogeneous and heterogeneous vegetation refers to amount of vegetation cover, not amount of vegetation type.

The goal of improving the detection of heterogeneous vegetation for mapping coastal vegetation was identified through remote sensing literature with researchers who noted inadequate detection, classification and mapping of heterogeneous land cover as a significant contributor to reduced classification accuracy (Asner and Heidebrecht 2002; Schmidtlein et al. 2007; Kearney et al. 2009). The objectives identified to meet this goal were (a) to quantify the relationship between vegetation cover and plant area index (PAI) values so that PAI values could be used as an indicator of vegetation cover amount, and, (b) to quantify the relationship between PAI values and hand-held spectral data to map changes in vegetation cover. This project used PAI values because the relationships between PAI values and vegetation biophysical characteristics (e.g., above ground biomass) are well documented in the literature (Anser et al. 2003; Leblanc et al. 2005; Soudani et al. 2006). PAI values were used instead of leaf area index (LAI) since PAI values take into account all of the phytomass rather than only the green phytomass associated with LAI values. PAI values were deemed important for the mapping of vegetation in this region which can transition from green to dark red (senescence) throughout the growing season. However, information from the literature that refers to LAI and remote sensing relationship can be used to inform results of PAI relationships based on vegetation change.

The second objective compared PAI values with visible and infrared spectra data collected in situ using a hand-held spectrometer. This experimental design was identified by Brook and Kenkel (2002) who advocated that researchers carefully examine the relationship between ground and spectral data for vegetation mapping near Hudson Bay. This "provides a highly robust and flexible approach to thematic mapping since the analyst is able to make informed choices at all stages of the decision-making process" (Brook and Kenkel 2002, 4774). If the results show a statistically significant difference between PAI values for the two vegetation zones, and a distinct relationship between PAI values and reflectance spectra for each zone, this provides informed decisions for classification of vegetation along the coast (the next step of the project).

Background

Geospatial data and tools have been used for mapping shorelines susceptible to slow erosion processes, rising water levels, and subarctic vegetation change (Stow et al. 2004; Maiti and Bhattacharya 2011; Ahmad and Lakhan 2012). However, these studies show that shoreline position is challenging to detect due to the dynamic nature of tides, changes in deposition and erosion landscapes due to sea ice, and the systematic temporal requirements of satellite-based image collection (Boak and Turner 2005; Maiti and Bhattacharya 2011). Thus indicators of shorelines are used in mapping projects to detect changes of shorelines over time.

Vegetation distribution along coastlines can be used as an indicator of shoreline position since vegetation has been found to be representative of changes in landscape ecological properties (Schmidt et al. 2004). Success in mapping coastal vegetation is obtained if the vegetation has homogeneous cover (e.g., 100% vegetation). Mapping vegetation based on spectral reflectance is based on characteristics such as plant tissue (leaf, woody stem, and standing litter), biochemistry, canopy biophysical properties (leaf and stem area, leaf and stem orientation, and foliage clumping), soil reflectance, illumination conditions and viewing geometry at time of image acquisition (Curran et al. 1992). For example, Schmidt and Skidmore (2003) mapped the distribution of vegetation of coastal wetlands while Kennedy (2012) mapped spatial and temporal changes in subarctic homogeneous vegetation.

Along the Hudson Bay coastline, the amount of vegetation cover decreases with proximty to the shoreline due to high soil and atmospheric salinity, strong coastal winds, and successive vegetation ridges from post-glacial uplift (Laliberté and Payette 2008). While homogeneous vegetation can be successfully mapped, the challenge is to map heterogeneous vegetation cover with better classification accuracy. Heterogeneous vegetation amounts result in image "mixel" where pixel reflectance values are a product of mixed land cover; in this case, coastal vegetation, sediment and rock (Asner and Heidebrecht 2002; Schmidtlein et al. 2007; Kearney et al. 2009). The variable proportions of vegetation, sediment and rock within an image pixel results in highly variable reflectance values within each pixel for heterogeneous vegetation (or any heterogeneous surface). The wide range of reflectance values will result in poor classifica-

tion accuracy because the traditional classification algorithms require unique and non-overlapping reflectance values for each land-cover class (Curran et al. 1992).

To overcome the poor classification of heterogeneous vegetation, researchers have suggested the use of spectral curve shape or spectral ratios from hyperspectral data. Figure 1a provides a schematic of the typical shape expected for a spectral curve of healthy, green vegetation. In Schmidt and Skidmore (2003), the ability to discriminate salt marsh vegetation was done using the shape properties of the spectral signature curve. The authors concluded that the ability to differentiate salt marsh species was maximized when the near-infrared (NIR) and short wave infrared wavelengths (740 to 1820 nm) were included in the classification. Schmidt and Skidmore (2003) state that the leading edge of the near-infrared (NIR) plateau was essential for discriminating salt marsh vegetation. The NIR plateau region appears after reflectance values increased from the red to the NIR region (Figure 1a).

To detect changes in vegetation, other researchers have developed indices using ratios of red and NIR reflectance values because these two values vary depending on plant health, amount and type. Simple ratio (SR), normalized difference vegetation index (NDVI) and soil adjusted vegetation index (SAVI) are all ratios that have been found to correlate with LAI values (Turner et al. 1999; Brown et al. 2000). Turner et al. (1999) concluded that use of these surface reflectance indices was far superior for vegetation discrimination when compared to digital number, radiance or top of atmosphere reflectance alone. Brown et al. (2000) used a modified SR vegetation index to investigate the potential of the shortwave infrared signal to improve LAI retrieval in the boreal forests of Canada. These results showed that red-NIR ratio values were vegetation-type, phenological and health dependent, and were most successful for broad leaf forest land cover and less successful for conifer forest, shrubland and grassland. The success of the modified SR was because it optimized the characteristic shape of vegetation spectral curve compared to using individual reflectance values of the visible and infrared wavelengths (Brown et al. 2000). The typical shape of vegetation spectral signature includes a dip in red spectra (low reflectance) followed by a steep increase in NIR reflectance (Figure 1a). Healthy vegetation has a steeper slope between the recorded red and NIR reflectance values because healthy vegetation reflects more NIR radiation.

Both Nemani et al. (1993) and Brown et al. (2000) found a large range in SR values associated with low LAI values and concluded that indices alone could not be used to estimate LAI in open forest canopies or low vegetation environments. Chen and Cihlar (1996) suggest that the scattered reflectance observed for low vegetation environments (low LAI values) would explain the variation in background reflectance from such vegetation and thus lower classification accuracies would result. The findings of Nemani et al. (1993) and Brown et al. (2000) are important for non-forested environments where heterogeneous land cover could yield analogous scattering issues.

To overcome the limitations of background reflectance on the red-NIR ratio relationships, researchers have proposed taking the first derivative of the spectral reflectance ratio index. The typical vegetation signature curve results in a slope from red to NIR reflectance (680 to 780 nm) that is known as the red edge (Figure 1a). When the vegetation curve is transformed using the first derivative of vegetation spectral curve, the red edge appears as a peak (Figure 1b) with the position and shape of the peak found to be affected by chlorophyll content and scattering properties of the vegetation (Horler et al. 1980; Boochs et al. 1990; Filella and Penuelas 1994). The characteristics that are used to improve vegetation mapping from the first derivative curve include the amplitude, area (Σ680 to 780 nm) and 725/702 nm ratio calculated from the average spectra data (Figure 1b). The amplitude is represented by the maximum value of the peak, the area is represented by the sum of the values from 680 nm to 780 nm, and the 725/702 nm ratio is the ratio between reflectance values in the NIR range which have been shown to be sensitive to vegetation stress and heterogeneity.

Advantages to using derivative spectra characteristics include a minimization of additive constants (e.g., illumination changes) and a reduction in the sensitivity to variable background reflectance (Curran et al. 1990; Imanishi et al. 2004; Kochubey and Kazantsev 2012). The first derivative technique has been applied to improve vegetation classification by overcoming interference from soil background reflectance or for resolving

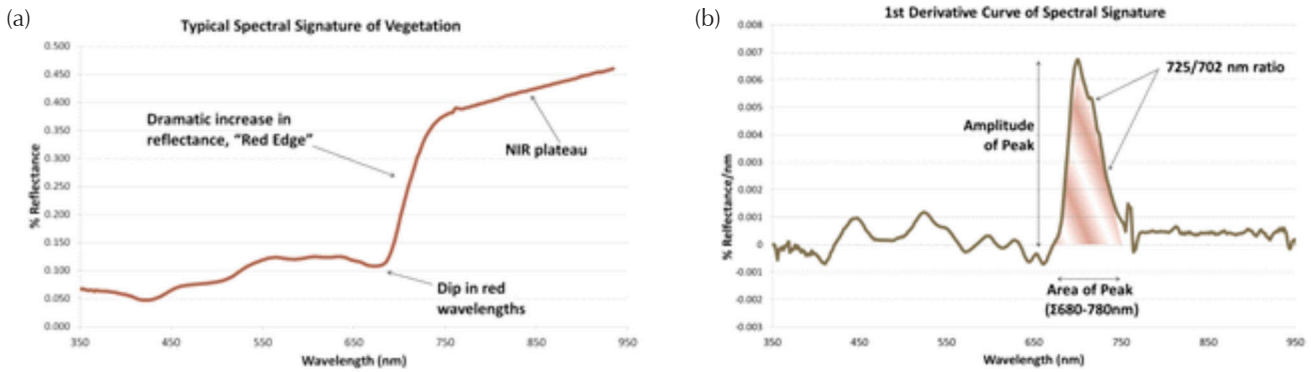

Figure 1
(a) Typical reflectance spectra of healthy vegetation within the study; and (b) the first derivative curve of the spectra from Figure 1(a)

complex spectra of several target species (Demetriades-Shah et al. 1990). Demetriades-Shah et al. (1990) showed that derivative spectral indices were superior to the conventional broadband spectral indices (e.g., SR, NDVI, SAVI) for monitoring chlorosis in vegetation. The position and shape of the first derivative peak has been found to be affected by chlorophyll content and scattering properties of the vegetation (Horler et al. 1980; Boochs et al. 1990; Filella and Penuelas 1994). The derivative peak has been used to measure chlorophyll content (Horler et al. 1980; Curran et al. 1990; Filella and Penuelas 1994; Gitelson et al. 1996), to monitor nitrogen stress (Boochs et al. 1990; Filella and Penuelas 1994) and drought (Filella and Penuelas 1994; Mano et al. 1999), and to identify sulphide stress (Collins et al. 1983) and areas of high vegetation damage (Rock et al. 1988).

Characteristics of the first derivative peak have also been found to be correlated with LAI values (Filella and Penuelas 1994; Danson and Plummer 1995). Filella and Penuelas (1994) found strong correlations between both the area and amplitude of the first derivative peak and LAI values. Danson and Plummer (1995) also observed a strong non-linear correlation between LAI values and the position of the first derivative peak. The area of the first derivative peak appears to better follow the evolution of LAI values (change in values from low to high based on vegetation biomass) compared to the amplitude of the peak. Filella and Penuelas (1994) concluded that the area of the first derivate curve was dependent only on the contrast of red and NIR reflectance values while the amplitude was also dependent on the amount of energy reflected in these two wavelength regions.

In addition to using the shape characteristics (amplitude, peak, area) of the first derivative curve, other researchers have incorporated ratios based on measured values found along this curve. Kochubey and Kazantsev (2007) proposed an index where the ratio of the two peak intensities, 725 nm and 702 nm, be computed and used to map vegetation. Although the peak wavelengths did not always coincide with maxima in the derivative plot, the 725/702 nm ratio did show the most reliable interrelation between chlorophyll contents and the derivative index (Kochubey and Kazantsev 2012). The authors found the 725/702 nm ratio was successful when tested against a variety of plant species and is computationally simple compared to identifying the maxima for each individual curve. Both Filella and Penuelas (1994) and Danson and Plummer (1995) related LAI values to first derivate characteristics or ratios in controlled experiment and forested regions, respectively. However, no work has been done on using characteristics of the first derivative curve for subarctic coastal vegetation.

Study site

The field work was conducted at Bird Cove (58° 47′N, 94° 11′W) close to the Churchill Northern Studies Centre (CNSC), which is situated approximately 20 km south-east of the town of Churchill, Manitoba. The study site is on the western edge of Hudson Bay and is situated near an estuary carrying freshwater from the southern plains and boreal forest (Figure 2). This creates a unique and fragile ecology in the region that is susceptible to climate change due to loss of permafrost, sea level rise and post-glacial isostactic rebound (Rouse et al. 1997). The heterogeneous zone along the western coast of Hudson Bay is an area

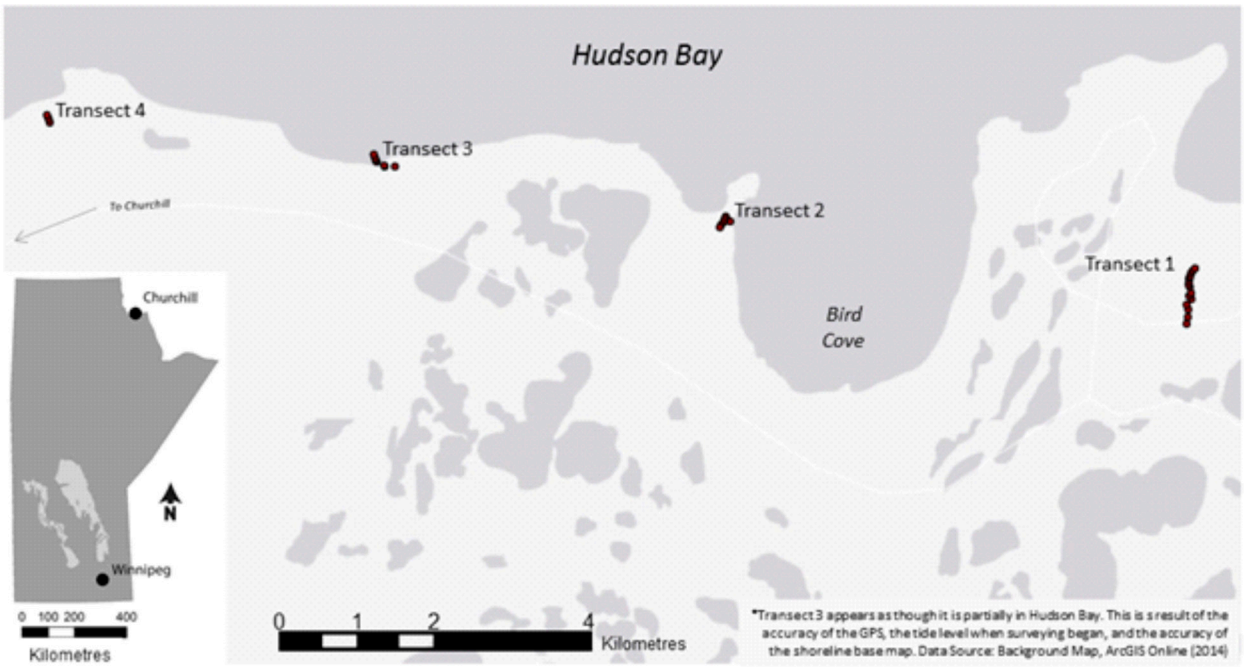

Figure 2
Bird Cove transects for in situ data collection, east of Churchill, Manitoba on Hudson Bay. (Map Data: ©2013 Esri, DeLorme, NAVTEQ, Survey Data from the authors)

several hundred metres wide that is characterized by a combination of geologic materials (sediment, rock), ponds and reduced vegetation cover approaching the bay. The Hudson Bay Lowlands region is underlain by calcareous Paleozoic limestone and dolomite, both considered soft rock with values of 3 to 4.5 on the Mohs hardness scale. These soft rocks experience significant erosion due to seasonal storms and annual sea ice advance and retreat (Ritchie 1957; Johnson et al. 1987).

This region was chosen because it represents the interface between the Arctic tundra, boreal forest and Arctic marine biomes. There are approximately 400 vascular plant species native to the Churchill area, including horsetails (*Equisetem* spp.), clubmosses (*Lycopodium* spp.), ferns, conifers, and flowering plants (Johnson et al. 1987). These species represent 17 vegetation communities found in the region with two, strand and salt marsh communities, existing within the study site. Homogeneous and heterogeneous vegetation cover was observed and quantified by Werner et al. (in press) with the vegetation zones corresponding with changes in vegetation percent cover, cover type, colour and texture.

Methods

The sites of four transects (Figure 2) were chosen for their accessibility, vegetation composition and safety. This study area is adjacent to "polar bear alley" so the four transects required good proximity to road/track access which allowed for a safety vehicle to be located nearby. Access to potential study sites was also limited by rock outcrops which prevented safe transport beyond these locations. The Bird Cove site is commonly used by CNSC researchers. Thus this project is contributing to the overall knowledge of the physical landscape of the area. In Figure 2, transect 3 appears to be floating in Hudson Bay. This is a result of the accuracy of the GPS unit (+/-10m) but also the accuracy of the shoreline position on the base map. This further emphasizes the need for more precise mapping of shoreline position as input into models.

Collection took place in late August 2012. Data collected from transects 1, 2 and 3 were used for the PAI values-vegetation zone analysis while transect 4 data was lost due to computer failure. In addition, limited battery life of the hand-held spectrometer meant that data were collected for only transects 1 and 3 for use in the PAI-spectra analysis. The transects varied in length from 202 m to 765 m with a maximum elevation of 9 m asl. Nineteen plots were sampled in the homogeneous zone and 13 in the heterogeneous zone. Although the heterogeneous region is of most importance for the current analysis, this zone represents a narrower swath of the coast resulting in a reduced number of plots compared to the homogeneous zone. To maximize the number of plots collected in the heterogeneous zone, a continuous sampling method was applied to capture the subtle changes in this narrow region (Werner et al. in press).

The biophysical variables collected in the field were chosen based on an understanding of the coastal environment and the ecological literature on the Hudson Bay Lowlands (McClure 1943; Ritchie 1957; Kershaw 1976; Johnson et al. 1987; Houle 1996; Imbert and Houle 2000; Brook 2001; Gagne and Houle 2002). Hemispherical photographs were collected so that PAI values could be generated to provide an indicator of percent cover for homogeneous and heterogeneous vegetation cover amounts. The hand-held spectra data were used to collect vegetation spectral reflectance across the visible and NIR wavelengths with the reflectance amounts for each wavelength being connected to form a spectral curve. The spectral curves for the vegetation regions were then transformed into first derivative spectra curves which allowed for the generation of shape characteristics (e.g., amplitude, area, and ratio).

In each 10 m x 10 m plot along the transects, hemispherical photographs and hand-held spectra data were collected in a z-pattern to ensure that the samples were random and representative of the vegetation within the plot (McCoy 2005). Hemispherical photographs were obtained using a Canon EOS60D camera with a Sigma 10 mm fisheye lens at a height of 0.95 m with an IFOV of 3.46 m^2. The photographs were sampled using a random walk method at transect 1, and this method was modified to account for red and green plant colour for the remaining three transects as plant colour change due to senescence is evident in late August in this area. The standard protocol of collecting eight hemispherical photographs within each plot was followed. These eight photographs were then input into CanEYE software to calculate true PAI values using the Miller formula (Miller 1967; EMMAH 2003).

Spectroscopy of the vegetation cover was collected using the ASD Fieldspec Pro at an angle of 0° facing downward perpendicular to the ground surface (ASD 2014a). The sensor subtended a viewing angle of 25° at a constant measure distance of 1.25 m for an instantaneous field of view (IFOV) of 0.28 m^2. The Fieldspec Pro unit averaged 500 counts per sample. A table was output from the ViewSpec Pro of the percentage reflectance per unit wavelength. An average curve of reflectance value for each plot was generated based on eight samples collected for each plot. From the average curve reflectance, the first derivative curve for each plot was then calculated using the RS^3 Spectral Acquisition Software (ASD Inc 2014b.). The first derivative characteristics include the amplitude, area (Σ680 to 780 nm) and 725/702 nm ratio of the first derivative peak.

Statistical correlations between PAI values for the vegetation zones were calculated using IBM SPSS Statistics 19. Characteristics of the first derivative curve were analysed using ROOT 5.34.02 (Brun and Rademakers 1997). A Z-test ($p=0.05$) was used to quantify the difference in PAI values between homogeneous and heterogeneous vegetation zones. The relationships between PAI values and first derivative spectral characteristics values were derived using regression analysis (Chen et al. 1997; Turner et al. 1999; Colombo et al. 2003).

Results and discussion

The first objective of this study was to determine if PAI values could be used as an indicator for differences in the homogeneous

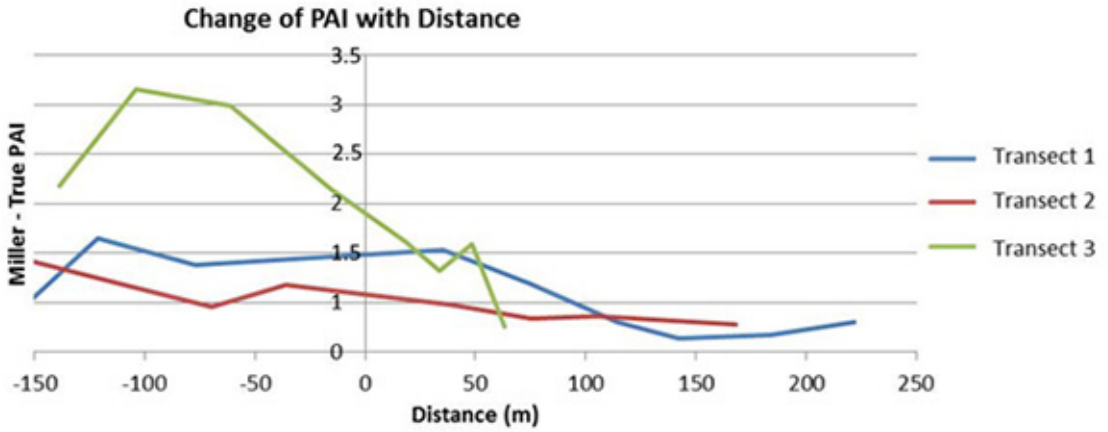

Figure 3
Change in PAI values relative to the boundary separating homogeneous and heterogeneous vegetation zones for transects 1 (blue), 2 (red) and 3 (green). The vertical line at 0 m represents the observed and quantified division between homogeneous and heterogeneous vegetation

and heterogeneous vegetation cover. The results showed there was a decline in PAI values from the homogeneous to the heterogeneous vegetation (Figure 3), which is particularly evident at the transition boundary. The PAI values pattern observed in Figure 3 corresponds with a decrease in vegetation cover (33% in salt marsh of transect 1; 10.5% in strand community of transect 3) from the homogeneous to the heterogeneous zone. In transect 1, when the sampling design did not account for vegetation colour, there were no significant differences obtained in PAI values between the homogeneous and heterogeneous vegetation cover (Table 1). In transects 2 and 3, when the sampling method did account for vegetation colour (red and green), there were statistically significant differences in PAI values between homogeneous and heterogeneous vegetation zones. Thus, PAI values can be used as an indicator of vegetation cover amount if colour is accounted for in the sampling and analysis.

The second objective was to quantify the relationship between PAI values and first derivative spectra characteristics to determine if the spectral data can be used to map the change from homogeneous to heterogeneous cover. The PAI values were plotted against the amplitude, area ∑680 to 780 and the 725/702 nm ratio data (Figure 4) based on n=273 field samples.

Table 1
Comparison of PAI values between homogeneous and heterogeneous vegetation

Transect	Sampling Design	Sample Size (n)	Z calculated (True PAI-Miller)	Z-Critical Value	Difference
Site 1	random	124	0.331	0.754	No
Site 2	stratified random	175	2.258	0.109	Yes
Site 3	stratified random	98	5.709	0.011	Yes

The results of the regression analysis showed that the relationship between PAI and first derivative spectra is dependent on the amount of vegetation cover. Figure 4 presents the results based on the homogeneous (left) and heterogeneous (right) vegetation cover amounts. In the heterogeneous zone, the strongest correlation was obtained for PAI values and the 725/702 nm ratio data (R^2= 0.931). In the homogeneous zone, the strongest relationship was obtained between PAI values and the amplitude data (R^2= 0.896). When considering both the homogeneous and heterogeneous zones, the amplitude characteristics of the first derivative curve resulted in the best overall results (R^2≈0.90 for both).

These results corroborate other literature which state that the characteristics of the first derivative peak is influenced by both chlorophyll and LAI/PAI variability (Boochs et al. 1990; Filella and Penuelas 1994). The findings of Filella and Penuelas (1994) also found a strong correlation between PAI values and the amplitude for some plants with variable water and nitrogen amounts. However, unlike Filella and Penuelas (1994), the results of this research did not show the area of the red edge peak as following the PAI evolution better than amplitude. The ratio is related to chlorophyll content of the vegetation (Kochubey and Kazantsev 2007). It is stated that the total phytomass (PAI) predicted with red and NIR indices will have a better relationship with vegetation than ratios that incorporate green wavelengths (Shippert et al. 1995; Riedel et al. 2005; Raynolds et al. 2006).

Although both homogeneous and heterogeneous vegetation cover have a strong correlation with first derivative characteristics, the observed direction of this relationship changed based on the percent cover categories. For homogeneous vegetation, there was a strong negative correlation between first derivative characteristics and PAI values, that is, higher PAI values were associated with lower spectral values (Figure 4). Conversely, in the heterogeneous vegetation, strong positive correlations between PAI values and first derivative characteristics were observed (Figure 4). Filella and Penuelas (1994) showed positive correlations for homogeneous vegetation cover. The PAI values should

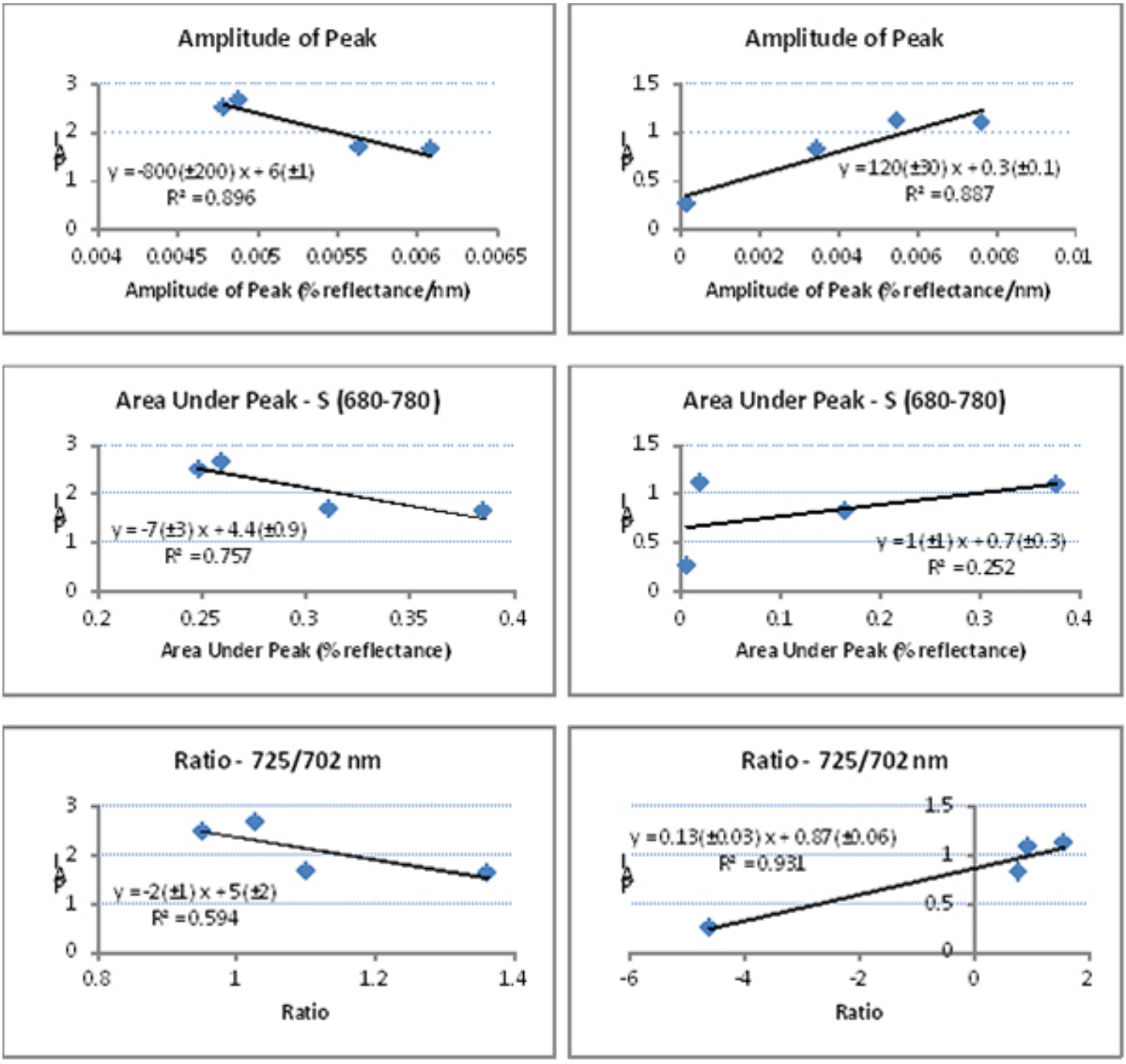

Figure 4
Relationships found between first derivative red edge peak characteristics (top-amplitude; middle-area; bottom-ratio) and PAI values for homogeneous cover (left) and heterogeneous cover (right)

rise with the increase in percentage of stem material in the canopy because of the decrease reflectance in the 680 nm due to chlorophyll absorption, and decreased magnitude but increased slope of the NIR plateau (Asner 1998). However, according to Danson and Plummer (1995), the difference in relationship direction may be attributed to strong non-linear relationships found between LAI values and first derivative amplitude values when a larger sample dataset is available.

Changes in vegetation species and change in sampling design in the two zones may also be potential reasons for the change in correlation direction. The vegetation transition boundary observed in the field was shown to be related to changes in plant species, percent cover and elevation based on Werner et al. (in press). An analysis of PAI values resulted in lower PAI values associated with the dominance of lichen, willow (*Salix* sp.) and sedges (*Carex* sp.) intermixed with bare ground or water. Higher PAI values were associated with willow, birch shrub and freshwater meadow marsh communities which consist almost entirely of vascular plants. These results are consistent with Brook and Kenkel (2002) who mapped Hudson Bay vegetation using traditional pixel-based methods. The change in sampling design from homogeneous (random) to heterogeneous (stratified random) may also contribute to the negative and positive correlations differences observed. The random sampling within the homogeneous zone resulted in larger variability in PAI values compared to PAI values in the heterogeneous zone. When the sampling was stratified, the regression relationships were stronger as the PAI values better represented the change in plant colour within the heterogeneous zone.

Conclusion

The results of this study showed that there were significant differences between PAI values collected in homogeneous versus heterogeneous subarctic coastal vegetation but only when the variation in plant colour is taken into consideration. Thus PAI values can be used as an indicator of plant cover amount when mapping homogeneous and heterogeneous vegetation differences. The differences in PAI values also independently validated the observed changes in homogeneous-heterogeneous vegetation found by Werner et al. (in press).

Once the difference in PAI values for homogeneous and heterogeneous zones was determined, the next step was to determine how the changes in PAI values were related with first derivative spectral curve characteristics. Strong linear relationships were found between PAI values and amplitude of the first derivative curve when the homogeneous and heterogeneous vegetation data were assessed separately. A strong positive correlation was found in the homogeneous zone compared to a strong negative correlation observed in the heterogeneous vegetation zone. The results of this project for coastal vegetation confirm those found in literature for experimental and forest applications. If hyperspectral data are available for mapping homogeneous and heterogeneous coastal vegetation, use of the first derivative amplitude will result is the best possible classification outcome (highest overall classification accuracy). Thus the next step of this project is to use hyperspectral image data to improve classification of the heterogeneous zone. This will allow for the identification of the homogeneous-heterogeneous boundary across space. Once identified, it can be used to more accurately georeference multi-temporal images for shoreline change detection.

References

Ahmad, S. R., and V. C. Lakhan. 2012. GIS-based analysis and modeling of coastline advance and retreat along the coast of Guyana. *Marine Geodesy* 35(1): 1–15.

ASD Inc. 2014a. ASD Fieldspec Pro by A PANalytical Company. http://discover.asdi.com/.

—. 2014b. Spectral Acquisition Software, ASD Inc. http://www.asdi.com/products/spectroscopy-software/rs3.

Asner, G. P. 1998. Biophysical and biochemical sources of variability in canopy reflectance. *Remote Sensing of Environment* 64(3): 234–253.

Asner, G. P., and K. B. Heidebrecht. 2002. Spectral unmixing of vegetation, soil and dry carbon cover in arid regions: Comparing multispectral and hyperspectral observations. *International Journal of Remote Sensing* 23(19): 3939–3958.

Asner, G. P., Scurlock, J. M. O., and J. A. Hicke. 2003. Global synthesis of leaf area index observations: Implications for ecological and remote sensing studies. *Global Ecology and Biogeography* 12(3): 191–205.

Bartlett, D. S., and V. Klemas. 1980. Quantitative assessment of tidal wetlands using remote sensing. *Environmental Management* 4(4): 337–345.

Boak, E. H., and I. L. Turner. 2005. Shoreline definition and detection: A review. *Journal of Coastal Research* 21(4): 688–703.

Boochs, F., G. Kupfer, K. Dockter, and W. Kühbauch. 1990. Shape of the red edge as vitality indicator for plants. *International Journal of Remote Sensing* 11(10): 1741–1753.

Brook, R. K. 2001. *Structure and dynamics of the vegetation in Wapusk National Park and the Cape Churchill Wildlife Management Area of Manitoba, Community and Landscape Scales*. Winnipeg, MB: University of Manitoba.

Brook, R. K., and N. C. Kenkel. 2002. A multivariate approach to vegetation mapping of Manitoba's Hudson Bay Lowlands. *International Journal of Remote Sensing* 23(21): 4761–4776.

Brown, L., J. M. Chen, S. G. Leblanc, and J. Cihlar. 2000. A shortwave infrared modification to the simple ratio for LAI retrieval in boreal forests: An image and model analysis. *Remote Sensing of Environment* 71(1): 16–25.

Brun, R. and F. Rademakers. 1997. ROOT - An object oriented data analysis framework. *Nuclear Instruments and Methods in Physics Research Section A: Accelerators, Spectrometers, Detectors and Associated Equipment* 389(1-2): 81–86.

Chen, J. M., and J. Cihlar. 1996. Retrieving leaf area index of boreal conifer forests using Landsat TM images. *Remote Sensing of Environment* 55(2): 153–162.

Chen, J. M., P. M. Rich, S. T. Gower, J. M. Norman, and S. Plum-

mer. 1997. Leaf area index of boreal forests: Theory, techniques, and measurements. *Journal of Geophysical Research* 102(D24): 29,429–29,443.

Collins, W., S.-H. Chang, G. L. Raines, F. Canney, and R. Ashley. 1983. Airborne biogeophysical mapping of hidden mineral deposits. *Economic Geology* 78(4): 737–749.

Colombo, R., D. Bellingeri, D. Fasolini, and C. M. Marino. 2003. Retrieval of leaf area index in different vegetation types using high resolution satellite data. *Remote Sensing of Environment* 86(1): 120–131.

Curran, P. 1980. Multispectral remote sensing of vegetation amount. *Progress in Physical Geography* 4(3): 315–341.

Curran, P. J., J. L. Dungan, and H. L. Gholz. 1990. Exploring the relationship between reflectance red edge and chlorophyll content in slash pine. *Tree Physiology* 7(1–2–3–4): 33–48.

Curran, P. J., J. L. Dungan, B. A. Macler, S. E. Plummer, and D. L. Peterson. 1992. Reflectance spectroscopy of fresh whole leaves for the estimation of chemical concentration. *Remote Sensing of Environmen*t 39(2): 153–166.

Danson, F. M., and S. E. Plummer. 1995. Red-edge response to forest leaf area index. *International Journal of Remote Sensing* 16(1): 183–188.

Demetriades-Shah, T. H., M. D. Steven, and J. A. Clark. 1990. High resolution derivative spectra in remote sensing. *Remote Sensing of Environment* 33(1): 55–64.

EMMAH. 2003. *Environnement Mediterranéen et Modélisation des Agro-Hydrosystèmes. CAN-EYE Imaging Software*. Rennes, France: National Institute of Agronomic Research (INRA). http://www6.paca.inra.fr/can-eye.

Filella, I., and Penuelas, J. 1994. The red edge position and shape as indicators of plant chlorophyll content, biomass and hydric status. *International Journal of Remote Sensing* 15(7): 1459–1470.

Gagne, J-M., and G. Houle. 2002. Factors responsible for *Honckenya peploides* (Caryophyllaceae) and *Leymus mollis* (Poaceae) spatial segregation on subarctic coastal dunes. *American Journal of Botany* 89(3): 479–485.

Gitelson, A. A., M. N. Merzlyak, and H. K. Lichtenthaler. 1996. Detection of red edge position and chlorophyll content by reflectance measurements near 700 nm. *Journal of Plant Physiology* 148(3–4): 501–508.

Horler, D. N. H., J. Barber, and A. R. Barringer. 1980. Effects of heavy metals on the absorbance and reflectance spectra of plants. *International Journal of Remote Sensing* 1(2): 121–136.

Houle, G. 1996. Environmental filters and seedling recruitment on a coastal dune in subarctic Quebec (Canada). *Canadian Journal of Botany* 74(9): 1507–1513.

Imanishi, J., Sugimoto, K., and Morimoto, Y. 2004. Detecting drought status and LAI of two *Quercus* species canopies using derivative spectra. *Computers and Electronics in Agriculture* 43(2): 109–129.

Imbert, É., and G. Houle. 2000. Persistence of colonizing plant species along an inferred successional sequence on a subarctic coastal dune (Québec, Canada). *Ecoscience* 7(3): 370–378.

Johnson, K. L., L. Fairfield, and R. R. Taylor. 1987. *Wildflowers of Churchill and the Hudson Bay Region*. Winnipeg, MN: Manitoba Museum of Man and Nature.

Kearney, M. S., D. Stutzer, K. Turpie, and J. C. Stevenson. 2009. The effects of tidal inundation on the reflectance characteristics of coastal marsh vegetation. *Journal of Coastal Research* 25(6): 1177–1186.

Kennedy, R. E. 2012. New views on changing Arctic vegetation. *Environmental Research Letters* 7(1): 1–3.

Kershaw, K. A. 1976. The vegetational zonation of the East Pen Island salt marshes, Hudson Bay. *Canadian Journal of Botany* 54(1–2): 5–13.

Kochubey, S. M., and T. A. Kazantsev. 2007. Changes in the first derivatives of leaf reflectance spectra of various plants induced by variations of chlorophyll content. *Journal of Plant Physiology* 164(12): 1648–1655.

—. 2012. Derivative vegetation indices as a new approach in remote sensing of vegetation. *Frontiers of Earth Science* 6(2): 188–195.

Laliberté, A-C., and S. Payette. 2008. Primary succession of subarctic vegetation and soil on the fast-rising coast of eastern Hudson Bay, Canada. *Journal of Biogeography* 35(11): 1989–1999.

Leblanc, S. G., J. M. Chen, R. Fernandes, D. W. Deering, and A. Conley. 2005. Methodology comparison for canopy structure parameters extraction from digital hemispherical photography in boreal forests. *Agricultural and Forest Meteorology* 129(3): 187–207.

McClure, H. E. 1943. Aspection in the biotic communities of the Churchill area, Manitoba. *Ecological Monographs* 13(1): 1–35.

Maiti, S., and A. K. Bhattacharya. 2011. A three-unit-based approach in coastal-change studies using Landsat images. *International Journal of Remote Sensing* 32(1): 209–229.

Mano, K., Y. Morimoto, and Y. Takigawa. 1999. Experimental study for estimation of leaf area index (LAI) and vigor using transmitted spectral properties. *Journal of the Japanese Institute of Landscape Architecture* 62(5): 543–546.

McCoy, R. M. 2005. *Field methods in remote sensing*. New York, NY: Guilford Press.

Miller, J. B. 1967. A formula for average foliage density. *Australian Journal of Botany* 15(1): 141–144.

Nemani, R., L. Pierce, S. Running, and L. Band. 1993. Forest ecosystem processes at the watershed scale: Sensitivity to remotely-sensed leaf area index estimates. *International Journal of Remote Sensing* 14(13): 2519–2534.

Raynolds, M. K., D. A. Walker, and H. A. Maier. 2006. NDVI patterns and phytomass in the circumpolar Arctic. *Remote Sensing of Environment* 102(3–4): 271–281.

Riedel, S. M., H. E. Epstein, D. A. Walker, D. L. Richardson, M. P. Calef, E. Edwards, and A. Moody. 2005. Spatial and temporal heterogeneity of vegetation properties among four tundra plant communities at Ivotuk, Alaska, U.S.A. *Arctic, Antarctic, and Alpine Research* 37(1): 25–33.

Ritchie, J. C. 1957. The vegetation of northern Manitoba II: A prisere on the Hudson Bay Lowlands. *Ecology* 38(3): 429–435.

Rock, B. N., Hoshizaki, T., and Miller, J. R. 1988. Comparison of in situ and airborne spectral measurements of the blue shift associated with forest decline. *Remote Sensing of Environment* 24(1): 109–127.

Rouse, W. R., M. S. V. Douglas, R. E. Hecky, A. E. Hershey, G. W. Kling, L. Lesack, P. Marsh, M. McDonald, B. J. Nicholson, N. T. Roulet, and J. P. Smol. 1997. Effects of climate change on the freshwaters of arctic and subarctic North America. *Hydrological Processes* 11(8): 873–902.

Schmidt, K. S., and A. K. Skidmore. 2003. Spectral discrimination of vegetation types in a coastal wetland. *Remote Sensing of Environment* 85(1): 92–108.

Schmidt, K. S., A. K. Skidmore, E. H. Kloosterman, H. van Oosten, L. Kumar, and J. A. M. Janssen. 2004. Mapping coastal vegetation using an expert system and hyperspectral imagery. *Photogrammetric Engineering and Remote Sensing* 70(6): 703–715.

Schmidtlein, S., P. Zimmermann, R. Schüpferling, and C. Weiß. 2007. Mapping the floristic continuum: Ordination space position estimated from imaging spectroscopy. *Journal of Vegetation Science* 18(1): 131–140.

Shippert, M. M., D. A. Walker, N. A. Auerbach, and B. E. Lewis. 1995. Biomass and leaf-area index maps derived from SPOT images for Toolik Lake and Imnavait Creek area, Alaska. *Polar Record* 31(177): 147–154.

Soudani, K., C. François, G. le Maire, V. Le Dantec, and E. Dufrêne. 2006. Comparative analysis of IKONOS, SPOT, and ETM+ data for leaf area index estimation in temperate coniferous and deciduous forest stands. *Remote Sensing of Environment* 102(1): 161–175.

Stow, D. A., A. Hope, D. McGuire, D. Verbyla, J. Gamon, F. Huemmrich, S. Houston, C. Racine, M. Sturm, K. Tape, L. Hinzman, K. Yoshikawa, C. Tweedie, B. Noyle, C. Silapaswan, D. Douglas, B. Griffith, G. Jia, H. Epstein, D. Walker, S. Daeschner, A. Petersen, L. Zhou, and R. Myeni. 2004. Remote sensing of vegetation and land-cover change in arctic tundra ecosystems. *Remote Sensing of Environment* 89(3): 281–308.

Turner, D. P., W. B. Cohen, R. E. Kennedy, K. S. Fassnacht, and J. M. Briggs. 1999. Relationships between leaf area index and Landsat TM spectral vegetation indices across three temperate zone sites. *Remote Sensing of Environment* 70(1): 52–68.

Werner, A., C. Enns, J. Storie, S. Fraser, J. Sewell, and G. Berard. in press. Biophysical characteristics of coastal vegetation in Bird Cove, Churchill, Manitoba. *Prairie Perspectives* 16.